Lipid-Derived Aldehydes Accelerate Light Chain Amyloid and Amorphous Aggregation†

Jorge Nieva,‡ Asher Shafton,§ Laurence J. Altobell III,§ Sangeetha Tripuraneni,§ Joseph K. Rogel,§ Anita D. Wentworth,§ Richard A. Lerner,§ and Paul Wentworth, Jr.*,§,||,⊥

Departments of Chemistry and Molecular and Experimental Medicine and The Skaggs Institute for Chemical Biology, The Scripps Research Institute, 10550 North Torrey Pines Road, La Jolla, California 92037, and The Scripps-Oxford Laboratory, Department of Biochemistry, University of Oxford, South Parks Road, Oxford OX1 3QU, U.K.

Received February 27, 2008; Revised Manuscript Received May 1, 2008

ABSTRACT: Antibody light chain (LC) aggregation *in vivo* leads to the systemic deposition of Ig light chain domains in the form of either amyloid fibrils (AL-amyloidosis) or amorphous deposits, light-chain deposition disease (LCDD), in mainly cardiac or renal tissue and is a pathological condition that is often fatal. Molecular factors that may contribute to the propensity of LCs to aggregate *in vivo*, such as the protein primary structure or local environment, are intensive areas of study. Herein, we show that the aggregation of a human antibody κ-(κ-MJM) and λ-(λ-L155) light chain (1 mg/mL) can be accelerated *in vitro* when they are incubated under physiologically relevant conditions, PBS, pH 7.4 and 37 °C, in the presence of a panel of biologically relevant lipid-derived aldehydes, 4-hydroxynonenal (4-HNE), malondialdehyde (MDA), glyoxal (GLY), atheronal-A (KA), and atheronal-B (ALD). Thioflavin-T (ThT) and Congo Red (CR) binding assays coupled with turbidity studies reveal that this aldehyde-induced aggregation can be associated with alteration of protein secondary structure to an increased β-sheet conformation. We observed that the nature of the conformational change is primarily dependent upon the lipidic aldehyde studied, not the protein sequence. Thus, the cholesterol 5,6-secosterols, KA and ALD, cause an amorphous-type aggregation which is ThT and CR negative for both the κ-MJM and λ-L155 light chains, whereas 4-HNE, MDA, and GLY induce aggregates that bind both ThT and CR. TEM analysis revealed that amyloid fibrils were formed during the 4-HNE-mediated aggregation of κ-MJM and λ-L155 light chains, whereas ALD-induced aggregates of these LCs where amorphous in nature. Kinetic profiles of LC aggregation reveal clear differences between the aldehydes, KA and ALD, causing a classic nucleated polymerization-type aggregation, with a lag phase (of ~150 h) followed by a growth phase that plateaus, whereas 4-HNE, MDA, and GLY trigger a seeded-type aggregation process that has no lag phase. In-depth studies of the 4-HNE-accelerated aggregation of κ-MJM and λ-L155 reveal a clear aldehyde concentration dependence and a process that can be inhibited by the naturally occurring osmolyte trimethylamine *N*-oxide (TMAO). Given these data, we feel our recently discovered paradigm of inflammatory aldehyde-induced protein misfolding may now extend to LC aggregation.

Light-chain deposition disease (LCDD)[1] and light chain (LC) amyloidosis are a heterogeneous group of diseases characterized by the deposition of monoclonal paraproteins as nonfunctional and toxic aggregates in tissue (*1*). LCDD is differentiated clinically from LC amyloidosis by the absence of Congo Red birefringence on histologic sections containing protein deposits and variations in the pattern of tissue deposition (*2, 3*). LC amyloidosis is the most common systemic amyloidosis observed in the United States and was the first of the "amyloidoses" (*4*) where the constituent protein of the amyloid was properly identified. Glenner and co-workers in 1980 identified Ig light chains in amyloid from a patient with primary systemic amyloidosis (*5, 6*). In AL-amyloidosis, deposition of monoclonal paraprotein occurs in renal, hepatic, peripheral neuronal, and cardiac tissue with death resulting typically 1−4 years after diagnosis (*1, 7–11*). These monoclonal immunoglobulins can also deposit as amorphous aggregates, basement membrane precipitates, or intracellular crystals as found in patients with myeloma

† This work was supported by the ALSAM Foundation (J.N.), The Skaggs Institute for Research (P.W.), and the NIH (P.W., NIA, AG028300).

* To whom correspondence should be addressed. Telephone: +1-858-784-2576. Fax: +1-858-784-7385. E-mail: paulw@scripps.edu; paul.wentworth@bioch.ox.ac.uk.

‡ Department of Molecular and Experimental Medicine, The Scripps Research Institute.

§ Department of Chemistry, The Scripps Research Institute.

|| The Skaggs Institute for Chemical Biology, The Scripps Research Institute.

⊥ Scripps-Oxford Laboratory, Department of Biochemistry, University of Oxford.

[1] Abbreviations: LCDD, light-chain deposition disease; AL, antibody light chain; V_L, light-chain variable domain; C_L, light-chain constant domain; Ig, immunoglobulin; ThT, thioflavin-T; PBS, phosphate-buffered saline; 4-HNE, 4-hydroxynonenal; MDA, malondialdehyde; GLY, glyoxal; KA, atheronal-A; ALD, atheronal-B; VEH, vehicle; TMAO, trimethylamine *N*-oxide; FCS, fetal calf serum; CR, Congo Red; LDL, low-density lipoprotein; Aβ, β-amyloid; IPA, 2-propanol; PrP, prion protein; PrP^C, cellular prion protein; PrP^{SC}, scrapie prion protein.

10.1021/bi800333s CCC: $40.75
Published on Web 06/26/2008

nephropathy, light-chain deposition disease (LCDD), and adult (acquired) Fanconi syndrome (*12, 13*). Generally, patients exhibit only one form of light chain deposition. However, there is at least one report of a patient exhibiting both LC amyloidosis and LCDD involving the same light chain (*14*). Studies have shown that, in patients with myeloma (cast) nephropathy and LCDD, κ-isotype LCs predominate, whereas in LC amyloidosis λ-isotypes are more prevalent. Most remarkably, it has been found that of the λ-proteins, the $V_\lambda 6$ subgroup dominates, a factor attributed by Wall and co-workers (*15*) as being related to an intrinsic thermodynamic instability of the human $\lambda 6$ protein. The exact length of the light chains in the deposits varies from small N-terminal proteolysis fragments (~5 kDa) to N-terminal variable domains (V_L, ~12.5 kDa, the most common form) all the way to the complete variable and constant domain light chains (V_LC_L, ~25 kDa) (*1*).

While the mechanisms of LC aggregation remain unclear, the process is generally associated with conditions that generate monoclonal LC overproduction, such as multiple myeloma. However, only 10−15% of myeloma patients develop deposition diseases (*1*). Thus, overproduction of light chains alone is not sufficient to cause the disorder, but rather it only occurs in individuals where the light chain is susceptible to misfolding and aggregation. Two plausible explanations have been put forward that may account for light chain aggregation propensity: primary structure and/or environmental factors. Numerous groups have studied the importance of the LC amino acid sequence on aggregation propensity, but at present there is still no model based on protein sequence alone that is capable of predicting aggregation propensity or disease manifestations (*15–18*). More recently, Stevens and co-workers (*19*) have shown that the local environment of the light chain may also contribute to its aggregation *in vivo*. They showed that noncovalent association of glycosaminoglycans (GAGs), such as heparin 16000 and chondroitin sulfate B and C, with V_L proteins accelerates amyloid formation.

Recently, we have discovered a process that we are studying in the context of a number of disease-related sporadic amyloidoses. We have shown that, *in vitro*, certain inflammatory-derived lipidic aldehydes, when adducted to proamyloidogenic proteins in their native state, can induce misfolding and aggregation of the native protein sequences (*20, 21*). Thus, we have shown that the cholesterol 5,6-secosterols atheronal-A and -B (KA and ALD, respectively), which are derived from oxidation of cholesterol by activated leukocytes, accelerate the *in vitro* misfolding of $apoB_{100}$, the protein component of low-density lipoprotein (LDL), under physiologically relevant conditions (Figure 1) (*20*). More recently, we have shown that 4-HNE, a major lipid peroxidation product of membrane lipids, KA, and ALD accelerate the *in vitro* amyloidogenesis of β-amyloid peptides (Aβ 1−40 and 1−42) leading to prefibrillar assemblies of Aβ (*21*) via a process that involves a site-specific modification of Aβ (*22*) and that KA and ALD accelerate the aggregation of α-synuclein leading to β-crossed fibril aggregates (*23*).

Herein, we show that aggregation of human antibody κ and λ light chains can be accelerated when incubated in the presence of a panel of biologically relevant lipid-derived aldehydes (4-HNE, MDA, GLY, KA, and ALD, Figure 1). Biophysical studies reveal that the aggregation can occur with

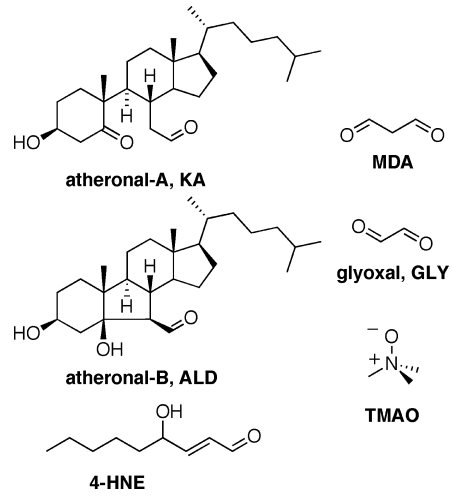

FIGURE 1: Molecules used in this study: atheronal-A (KA), atheronal-B (ALD), 4-hydroxynonenal (4-HNE), malondialdehyde (MDA), glyoxal (GLY), and trimethylamine *N*-oxide (TMAO).

modification of protein secondary structure to increased β-sheet content with some aldehydes, whereas others result in aggregation without affecting the β-sheet component of secondary structure. TEM analysis of the aldehyde-initiated aggregates reveals that the light chains may form either fibrillar or amorphous morphologies, dependent upon the aldehyde trigger. We further show that this aldehyde-initiated LC aggregation can be completely inhibited by coincubation with the naturally occurring osmolyte trimethylamine *N*-oxide (TMAO). Thus our paradigm, inflammatory aldehyde-accelerated misfolding of proteins, may have relevance in antibody light chain (LC) misfolding disorders.

MATERIALS AND METHODS

Congo Red (CR), glyoxal (GLY), malondialdehyde (MDA), and trimethylamine *N*-oxide (TMAO) were supplied by Sigma-Aldrich, 4-hydroxynonenal (4-HNE) by Calbiochem, and thioflavin-T (ThT) by Acros. Atheronal-A (3β-hydroxy-5-oxo-5,6-secocholestan-6-al) and atheronal-B (3β-hydroxy-5β-hydroxy-B-norcholestane-6β-carboxaldehyde) were synthesized as previously described (*20*).

Isolation, Purification, and Characterization of Human Immunoglobulin Light Chains: κ Light Chain (κ-MJM). Human light chain κ-MJM was obtained from a therapeutic apheresis specimen from a patient with Waldenstrom's macroglobulinemia and who had no known LC amyloidosis or LCDD. The Scripps Office for the Protection of Research Subjects approved the human subject's protocol. The patient's plasma was dialyzed against distilled water (3×) and centrifuged (10000 rpm, SORVAL). The pellet was then resuspended in phosphate-buffered saline (PBS, pH 7.4) and dialyzed against PBS. Plasma IgM was purified by gel electrophoresis (Sephacryl S-300 26/60 column) in PBS overnight at a rate of 1 mL/min. IgM fractions were identified by SDS−PAGE, pooled, and dialyzed in PBS. Purified IgM (50−100 mg) was then aliquoted into Eppendorf tubes, treated with 1% dithiothreitol (Fisher), and incubated at 37 °C for 1 h. The reduction was quenched by addition of iodoacetamide (100 μL, 0.75 M) followed by stirring at 25 °C for 30 min. Sample tubes were then pooled and dialyzed against urea (Pierce) (2 M, pH 2.8). Free κ-MJM was then purified by gel filtration chromatography (Sephacryl S-75

26/60 column) with urea (2 M, pH 2.8) buffer (0.5 mL/min). LC fractions were identified by SDS−PAGE, neutralized with an equal volume of Tris (1 M, pH 9), pooled, and then dialyzed into PBS (pH 7.4). Purity of the final product was >98% as confirmed by SDS−PAGE analysis with silver staining. Subsequent protein concentrations were determined by absorbance at 280 nm using the following equivalence: [κ-MJM] (in mg/mL) = OD_{280}/1.23 and $\epsilon_{280} = 2.90 \times 10^4$ M^{-1} cm^{-1} (as determined by BCA analysis and confirmed by measurement of dry weight). MW = 23540 Da as measured by MALDI MS. The isotype was confirmed as κ using an isotyping kit (Sigma).

Isolation, Purification, and Characterization of λ Immunoglobulin Light Chain λ-L155. Human light chain λ-L155 was obtained from cultured human plasmacytoma cells (ATCC No. CCL-155) (*2425*), grown in high density in RPMI 1640 supplemented with L-glutamine (2 mM), HEPES (10 mM), sodium pyruvate (1 mM), glucose (4.5 g/L), bicarbonate (1.5 g/L), and 10% FCS. The cultures were centrifuged, and the supernatant was concentrated through a 10K membrane and purified by gel filtration chromatography (Sephacryl S-200 26/60 column) in PBS (0.2 mL/min). Light chain fractions were identified by SDS−PAGE (10−15% gels) and confirmed by ELISA. These fractions were then pooled, concentrated, dialyzed in phosphate buffer (PB, 20 mM, pH 7.0), and further purified by passage through a HiTrap Blue HP column (Amersham No. 17-0412-01, 15 mL). Protein samples were then pooled, concentrated, and repurified on a Sephacryl S-200 26/60 column (0.2 mL/min). Pooled protein fractions were then dialyzed into PBS (pH 7.4). Final purity of the light chain λ-L155 was >98% as confirmed by SDS−PAGE with silver staining. Protein concentration was determined by OD at 280 nm using the following equivalence: [λ-L155] (in mg/mL) = OD_{280}/1.39 and $\epsilon_{280} = 3.22 \times 10^4$ M^{-1} cm^{-1} (as determined by BCA analysis and confirmed by measurement of dry weight). MW = 23160 Da as measured by MALDI MS. The isotype was confirmed as λ using an isotyping kit (Sigma).

Aggregation Assays. Aggregation reactions were initiated by addition of the test compound (4-HNE, MDA, GLY, KA, ALD) at specified concentrations in 2-propanol (IPA) to the antibody light chains (λ-L155 or κ-MJM at 1 mg/mL, 43 and 42 μM, respectively, unless otherwise stated) in PBS (pH 7.4) (final organic solvent component was 0.1%). All assays were performed in Eppendorf microcentrifuge tubes at 37 °C. Each solution was equilibrated to 37 °C before mixing. Assay volumes were 500 μL unless otherwise stated. After the initial mixing, assays were agitated gently on a Waveline rotator (10 rpm). Control experiments comprising of LC alone, bovine serum albumin (BSA) and compound, and compound alone were always performed in parallel.

ThT Binding and Fluorescence. Aggregation assays were prepared as described above. At times throughout the aggregation assay, aliquots (10 μL) were removed and added to a solution of ThT in water (240 μL, 20 μM) and incubated for 10 min at room temperature. ThT fluorescence was then measured on a Molecular Devices Spectramax Gemini XS micotiter plate spectrofluor-meter, in 96-well black bottom polystyrene microtiter plates, with excitation at 440 nm (2 nm bandwidth) and emission at 485 nm (5 nm bandwidth). Data points are reported as the mean value ± SEM of at least duplicate measurements.

Turbidity. Aggregation assays were prepared as described above with reaction volumes being 1 mL. At times during the incubation aliquots (100 μL) were removed and added to a microtiter plate. Turbidity was monitored at 400 nm on a Molecular Devices SpectramaxPlus microtiter plate reader. Data points are reported as the mean value ± SEM of at least duplicate measurements.

Congo Red (CR) Binding. CR solutions were prepared as described by Klunk et al. (*26*). In brief, a stock solution of CR (300 μM) was prepared in PBS (pH 7.4) containing ethanol (10% v/v). This solution was filtered through a 0.2 μm filter and stored at 4 °C. Concentrations of CR were determined by measuring the absorbance of solutions at 505 nm. For CR binding assays the LC aggregation experiments were prepared as described above. At times throughout the assay, aliquots (10 μL) were removed and added to a CR solution (90 μL, 10 μM) in ethanol (10% v/v) and incubated for 20 min at room temperature. Absorbance spectra were recorded on a UV/visible spectrophotometer (Molecular Devices Spectramax Plus) in 96-well microtiter polystyrene plates from 300 to 800 nm (every 2 nm). Each reported spectrum is the mean of six absorbance spectra scanned at each time point. Spectra are generally reported uncorrected unless otherwise stated. In the case where corrected spectra are reported, these spectra have been corrected for the light scatter caused by the LC alone and are prepared by subtraction of the absorbance spectra of the LC in the absence of CR from the spectra of the LC + CR.

Far-UV Circular Dichroism. Aggregation assays were prepared as described above, and CD measurements were made in an AVIV 202-SF CD spectrometer (AVIV instruments) in the amide band (190−240 nm) at a protein concentration of 1.0 mg/mL in cells with a 1 cm path length at a scan speed of 20 nm/min with a 1 nm bandwidth and a 4 ms response. The spectra were prepared 10-fold, averaged, and baseline corrected by subtraction of a blank buffer (PBS, pH 7.4, 0.1% IPA). These far-UV CD spectra were then analyzed on the DichroWeb Web site (*27, 28*) using CDSSTR (*29*) and SELCON3 (*30*) algorithms.

Transmission Electron Microscopy. Parlodion-coated copper grids (200 mesh) were glow discharged and immediately inverted onto 4 μL droplets of each sample on a sheet of Parafilm. Following a 2 min incubation at room temperature, the excess liquid was removed using a Whatman filter paper, and each grid was inverted onto a droplet of aqueous uranyl acetate (2% w/v) for 2 min. The excess liquid was removed and the grid allowed to dry fully. The grids were examined on a Philips CM100 electron microscope (FEI, Hillsbrough OR). Images were documented using Kodak SO163 EM film. Negatives were scanned at 600 lpi (lines per inch) using a Fuji FineScan 2750 and converted to TIF format for subsequent analysis in Adobe Photoshop CS.

RESULTS

Aggregation of LC κ-MJM Monitored by ThT Fluorescence. The fluorescence emission of the dye ThT is increased upon binding to protein aggregates with a cross-β-sheet structure (*31*), either fibrillar or nonfibrillar in morphology (*21, 32*). This change in ThT fluorescence is a convenient and generally accepted method for following the kinetics of amyloid formation. Thus, we compared the time-dependent

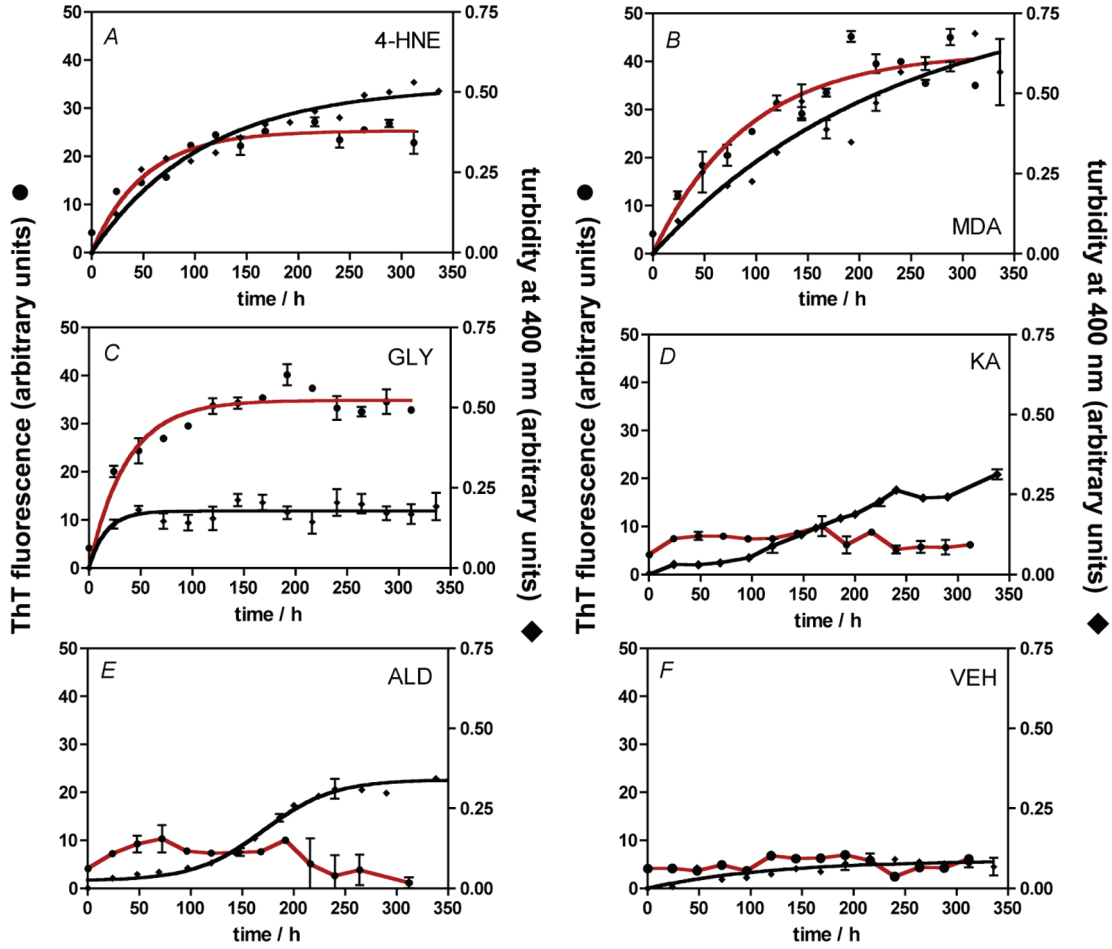

FIGURE 2: Aggregation of human LC κ-MJM as measured by ThT fluorescence (left *Y*-axis, ●) and turbidity (right *Y*-axis, ◆). The human AL-κ-MJM (1 mg/mL, 42 μM) in PBS (pH 7.4) was incubated at 37 °C with the lipidic aldehydes (each at 100 μM) (A) 4-HNE, (B) MDA, (C) GLY, (D) KA, and (E) ALD or with vehicle (F) VEH PBS with 0.1% IPA. At times throughout the assay, aliquots were removed and either the aliquots were added to a ThT solution (20 μM) in water and the fluorescence was measured (excitation, 440 nm; emission, 485 nm) or the turbidity of the solution was measured (400 nm). Data are reported as the mean ± SEM for at least duplicate measurements.

changes in ThT fluorescence (excitation, 440 nm; emission, 485 nm) of solutions of the human AL, κ-MJM (1 mg/mL, 42 μM), incubated in phosphate-buffered saline (PBS, pH 7.4) at 37 °C for up to 300 h, with either vehicle (VEH, PBS with 0.1% IPA) or in the presence of the biologically relevant aldehydes, 4-HNE, MDA, GLY, KA, and ALD (each at 100 μM) (Figure 2). A time-dependent increase in ThT fluorescence occurs during incubation with 4-HNE, MDA, and GLY to the light chain κ-MJM (Figure 2A−C). In contrast, there was no significant increase in the ThT fluorescence of the LC κ-MJM when incubated with KA or ALD or with vehicle (VEH) during the same time course. No increase in ThT fluorescence was observed with bovine serum albumin (BSA) treated with 4-HNE, MDA, GLY, KA, and ALD (each at 100 μM) (data not shown). Thus, 4-HNE, MDA, and GLY (each at 100 μM) seem to be accelerating the formation of an amyloid aggregate of this human AL, κ-MJM under physiologically relevant conditions (PBS, pH 7.4), relevant to control.

Interestingly, there is no lag phase in the ThT fluorescence profiles of the aggregation of κ-MJM with 4-HNE, MDA, and GLY; rather the increase in fluorescence is immediate and reaches a maximum at a time point and fluorescence amplitude that is dependent upon the aldehyde being studied (Figure 2A−C). The quasi-exponential time course observed for the 4-HNE-, MDA-, and GLY-accelerated κ-MJM amyloid formation is more representative of a "seeded" or so-called downhill polymerization than the quasi-sigmoidal profile expected for a classical unseeded nucleation-dependent aggregation process (*33, 34*) and is in line with what we observed with the seeded polymerization effect induced by KA, ALD, and 4-HNE with amyloid-β(1−40) and amyloid-β(1−42) (*21*).

Aggregation of LC κ-MJM Monitored by Turbidity. There is a time-dependent increase in the turbidity of the solutions of human LC κ-MJM (1 mg/mL) (as measured by the absorbance of the aggregation solution at 400 nm) when incubated with 4-HNE, MDA, GLY, KA, and ALD (each at 100 μM) but not when incubated with VEH (PBS with 0.1% IPA), the profile of turbidity change being dependent upon the aldehyde studied (Figure 2). The time course of the turbidity change for 4-HNE and MDA was similar to their respective kinetic changes in ThT fluorescence increase observed with these aldehydes, i.e., an immediate increase in turbidity (no observable lag phase), suggestive of a seeded polymerization mechanism, that reaches a maximum (Figure 2A,B). The one significant difference between the turbidity and ThT fluorescence profiles induced by these aldehydes is that the turbidity lags behind the ThT fluorescence, such that the 4-HNE-induced ThT maximum is reached at ∼125 h, whereas the turbidity maximum is reached at ∼250 h (Figure 2A). For MDA,

the ThT fluorescence maximum is reached at ~200 h, and the turbidity asymptote has not been reached by 310 h (the end of the experiment). That the turbidity lags behind the ThT fluorescence is not surprising when one considers that turbidity by necessity is a measure of higher order aggregates; i.e., ThT is a more sensitive probe for assembly of amyloid-like quaternary structure.

During incubation of κ-MJM with the dialdehyde GLY, the turbidity profile of the aggregation solution increases to a plateau at 50 h that does not change through the course of the experiment (up to 350 h). In fact, the turbidity maximum is reached faster than the ThT fluorescence, which itself continues to rise until ~150 h into the assay, suggesting that the main form of the GLY-κ-MJM aggregate, that exhibits ThT binding, is not as insoluble as the aggregate formed between κ-MJM and 4-HNE and MDA.

The turbidity of the solutions of κ-MJM during incubation with the cholesterol 5,6-secosterols KA and ALD exhibits a lag phase, which lasts ~100 h, followed by a rise in turbidity that asymptotes at ~250 h (Figure 2D,E). This kinetic profile is very much in line with a "nucleated polymerization" process. As detailed *vide supra*, neither KA nor ALD incubation with κ-MJM led to an increase in ThT binding, suggesting that the κ-MJM aggregates triggered by KA and ALD are not amyloid-like.

Aggregation of LC κ-MJM Monitored by Congo Red (CR) Binding. CR is a diazo dye that binds with high specificity to proteins that have significant amounts of β-sheet secondary structure. Proteins that lack or contain only a minor amount of β-sheet do not bind CR whereas protein quaternary assemblies that are comprised of parallel or antiparallel β-sheet exhibit high binding of CR and, in doing so, perturb the absorbance profile of the diazo dye (*26*). The CR absorbance profiles of CR (10 μM) were measured upon addition to κ-MJM (1 mg/mL, 42 μM) in PBS (pH 7.4) that had been incubated with 4-HNE, MDA, GLY, ALD (each at 100 μM), and VEH for either 1 min or 300 h (Figure 3). A red spectral shift in the absorbance spectrum of CR, characteristic of CR binding to amyloid, was observed for the long-term incubation of κ-MJM with the aldehydes 4-HNE, MDA, and GLY (Figure 3A−C) but not ALD or VEH (data not shown). These data for CR binding to κ-MJM treated with aldehydes are supportive of the data for ThT binding in that the aldehydes 4-HNE, MDA, and GLY induce a κ-MJM aggregate that is amyloid-like in structure, whereas the secosterol ALD induces an aggregate that is not amyloid-like.

The combined data, ThT-binding, CR-binding, and turbidity, suggest that these inflammatory aldehydes accelerate the formation of aggregates of this human κ-MJM antibody light chain, relative to control, and that the aggregates formed can be either amyloid-like or non-amyloid.

Aggregation of LC λ-L155 Monitored by ThT Fluorescence. The time-dependent changes in ThT fluorescence (excitation, 440 nm; emission, 485 nm) were measured of solutions of the human AL, λ-L155 (1 mg/mL, 43 μM), incubated in PBS (pH 7.4) at 37 °C with either VEH (PBS and 0.1% IPA) or in the presence of the aldehydes 4-HNE, MDA, GLY, KA, and ALD (each at 100 μM) (Figure 4). A time-dependent increase in ThT fluorescence is observed upon addition of 4-HNE, MDA, and GLY to the light chain λ-L155. There is no clear lag phase in the ThT fluorescence

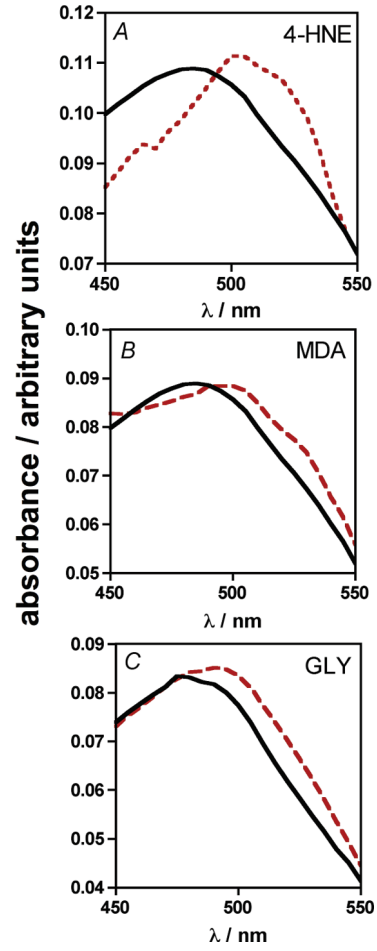

FIGURE 3: Spectral characteristics of Congo Red bound to κ-MJM after incubation with a panel of lipidic aldehydes. Corrected absorbance spectra (450−550 nm) of solutions of CR (81 μM) and κ-MJM (0.09 mg/mL) during incubation [t = 0.06 (—) and 300 h (---)] with (A) 4-HNE, λ_{max} 0.06 h = 485 nm, 300 h = 505 nm, (B) MDA, λ_{max} 0.06 h = 485 nm, 300 h = 500 nm, and (C) GLY, λ_{max} 0.06 h = 485 nm, 300 h = 500 nm. There was no change in absorbance spectra (450−550 nm) of solutions of CR and κ-MJM (0.09 mg/mL) when incubated with ALD or VEH up to 300 h (data not shown).

profile of the LC with these three aldehydes; rather the increase is immediate and rises to a plateau. The plateau for GLY is reached at ~50−75 h, for 4-HNE at ~225−250 h, and for MDA at ~25−275 h. There was no significant increase in the ThT fluorescence of λ-L155 when incubated with KA, ALD, or vehicle (VEH). A major difference between the aldehyde-induced aggregation of λ-L155 and κ-MJM was that even though the absolute numbers of the ThT fluorescence for each of the three aldehydes are higher with λ-L155 than with κ-MJM, there was no observable turbidity in any of these solutions (data not shown).

Morphology of the 4-HNE- and ALD-Induced κ-MJM and λ-L155 Deposits. The aldehyde-induced LC aggregates were examined using transmission electron microscopy (TEM) (Figure 5). The aggregates were generated by incubation of either 4-HNE or ALD (100 μM each) with either κ-MJM and λ-L155 (1.5 mg/mL) for 160 h at 37 °C in PBS, pH 7.4 (0.1% IPA). The protein samples were then centrifuged (14000 rpm, 5 min), and the aggregates were analyzed by TEM. This analysis revealed that there is a clear difference in the morphologies of the κ-MJM and λ-L155 protein deposits induced by the two aldehydes. In the presence of

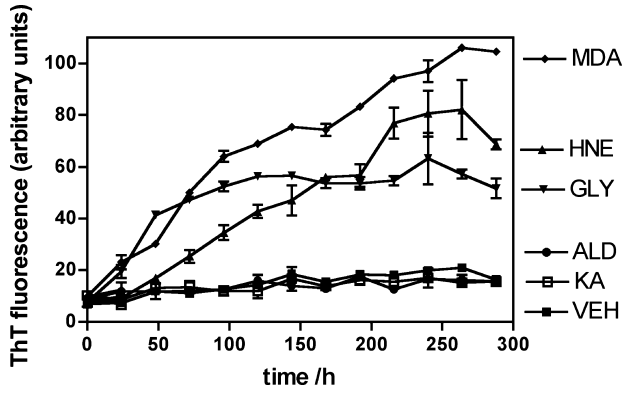

FIGURE 4: Aggregation of human LC λ-L155 as measured by ThT fluorescence. The human AL-λ-L155 (1 mg/mL, 43 μM) in PBS (pH 7.4) was incubated at 37 °C with the lipidic aldehydes (each at 100 μM) 4-HNE (▲), MDA (◆), GLY (▼), KA (□), and ALD (●) or with vehicle VEH (■) (PBS with 0.1% IPA). At times throughout the assay, aliquots were removed and added to a ThT solution (20 μM) in water, and the fluorescence was measured (excitation, 440 nm; emission, 485 nm). Data are reported as the mean ± SEM for at least duplicate measurements. Please note that under these conditions no turbidity was detected during any of the aggregation assays with the LC λ-L155.

ALD, the V_κ protein forms flat amorphous aggregates with a cross-sectional thickness of ~50 nm and indeterminate length (Figure 5B) and the V_λ protein forms loosely packed spherical amorphous aggregates, either individually or aggregated into more complex assemblies (Figure 5D). In the presence of 4-HNE, both the κ-MJM and λ-L155 assemble into a classical fibrillar morphology, a network of narrow diameter unbranched filaments (>1 μm in length) (Figure 5A,C).

4-HNE-Triggered LC Aggregation Is Concentration-Dependent. When the human LCs, either κ-MJM or λ-L155 (2 mg/mL, 80 μM), are incubated with varying concentrations of 4-HNE (0, 10, 50, 100, and 200 μM) in PBS (pH 7.4) and 37 °C with mild agitation, there is a 4-HNE concentration-dependent increase in β-sheet formation observed, as measured by ThT fluorescence and increase in CR binding (Figure 6A−C). An increase in ThT fluorescence, relative to treatment with VEH (PBS, 0.1% IPA), is observed at concentrations of ≥50 μM 4-HNE for the κ-MJM (Figure 6A) and ≥100 μM with the λ-L155 (Figure 6B). In the aggregation experiment with the λ-L155 light chain there was a small, but measurable increase in ThT fluorescence during incubation with the VEH. The kinetic profile for the VEH-induced aggregation was quasi-sigmoidal in nature and was typical of a nucleated polymerization, with a lag phase of ~100 h, a logarithmic growth phase, and a plateau phase that was reached at ~200 h. Interestingly, as the 4-HNE concentration is increased and the aggregation induced by 4-HNE increases, this kinetic profile changes to one of a seeded-type aggregation profile (Figure 6B). The CR binding of the protein κ-MJM after 4-HNE treatment mirrored the ThT fluorescence data, in that there was an increase in binding of CR and the red shift in the λ_{max} (from 490 to 505 nm) at concentrations of 4-HNE above 40 μM (Figure 6C). Circular dichroism spectra (CD) analysis of κ-MJM (1.0 mg/mL) treated with either VEH or 4-HNE (200 μM) for 160 h reveals that the far-UV CD of VEH-treated κ-MJM at pH 7.4 has a distinct negative molar elipticity minimum at 216 nm, in line with that expected for an immunoglobulin fold protein that is composed of a high proportion of β-structure. Incubation of κ-MJM with 4-HNE leads to significant changes in the AL's far-UV CD profile, with a reduction in the amplitude of the negative elipticity at 216 nm and a shift in its minima to 219 nm being observed (Figure 6D). These CD changes are attributed to the aggregated protein's secondary structure being a mixture of β-sheet and random coil, indicating a 4-HNE-induced loss of the native κ-MJM β-structure. However, a shift from 216 to 219−220 nm has been observed in the CD spectrum of β_2-microglobulin (*35*) during fibril formation, and given the ThT and TEM data of 4-HNE-induced aggregation of κ-MJM *vide supra*, this same phenomenon could be responsible for the shift in the minima observed.

AL-κ-MJM Aggregation Induced by 4-HNE Is Prevented by Trimethylamine N-Oxide (TMAO). Incubation of the human light chain of κ-MJM (1 mg/mL, 42 μM) with 4-HNE (100 μM) at 37 °C and pH 7.4 leads to a time-dependent increase in ThT fluorescence, turbidity, and CR binding (Figure 7). These increases in ThT fluorescence, turbidity, and CR binding are completely prevented when κ-MJM (1 mg/mL, 42 μM) is coincubated with 4-HNE (100 μM) and the osmolyte TMAO (0.5 mM).

A number of studies have shown that low molecular weight compounds can reverse or prevent the mislocalization and/or aggregation of proteins associated with human disease. These molecules, that include polyols such as glycerol and trimethylamines such as TMAO, have been called "chemical chaperones" and in cases where they occur naturally are termed osmolytes (*36*). Tatzelt and co-workers (*37*) have shown that TMAO can prevent scrapie formation *in vitro* by minimizing the conversion of PrP^C into PrP^{Sc}. Daggert and co-workers (*38*) subsequently showed that TMAO functions to stabilize PrP protein secondary structure indirectly through unfavorable enthalpic interactions of TMAO-influenced water.

DISCUSSION

Peroxidation of polyunsaturated fatty acids (PUFAs) in biological systems is always accompanied by the formation of aldehydic products (*39*). Since their original discovery, it has become evident that such lipid-derived aldehyde products are biologically active and can produce pathological effects *in vivo*. For example, 4-HNE, generated mainly from the peroxidation of ω-6 PUFAs, is cytotoxic, genotoxic, and mutagenic (*40*) and has been implicated in aging (*41*). It is known to disrupt mitogen-activated protein kinase pathways (*42, 43*) and impair the function of both nuclear factor-κB (*44*) and platelet-derived growth factor-β (*45*). Plasma concentrations of 4-HNE of 3−15 μM have been measured in healthy individuals (*46*) and are higher in diseases associated with high levels of oxidative stress, such as autoimmune diseases (*47*), hemodialysis (*48*), and other disorders associated with systemic inflammation. Local concentrations at sites of inflammation may be even higher. Malondialdehyde (MDA), generated from either peroxidation of PUFAs (ω-3, ω-6, and ω-9) or prostaglandin biosynthesis, is mutagenic and causes ROS imbalance by sequestration of glutathione. Glyoxal (GLY), generated during normal cellular metabolism from a number of enzyme-independent pathways, such as the Maillard reaction, sugar autoxidation,

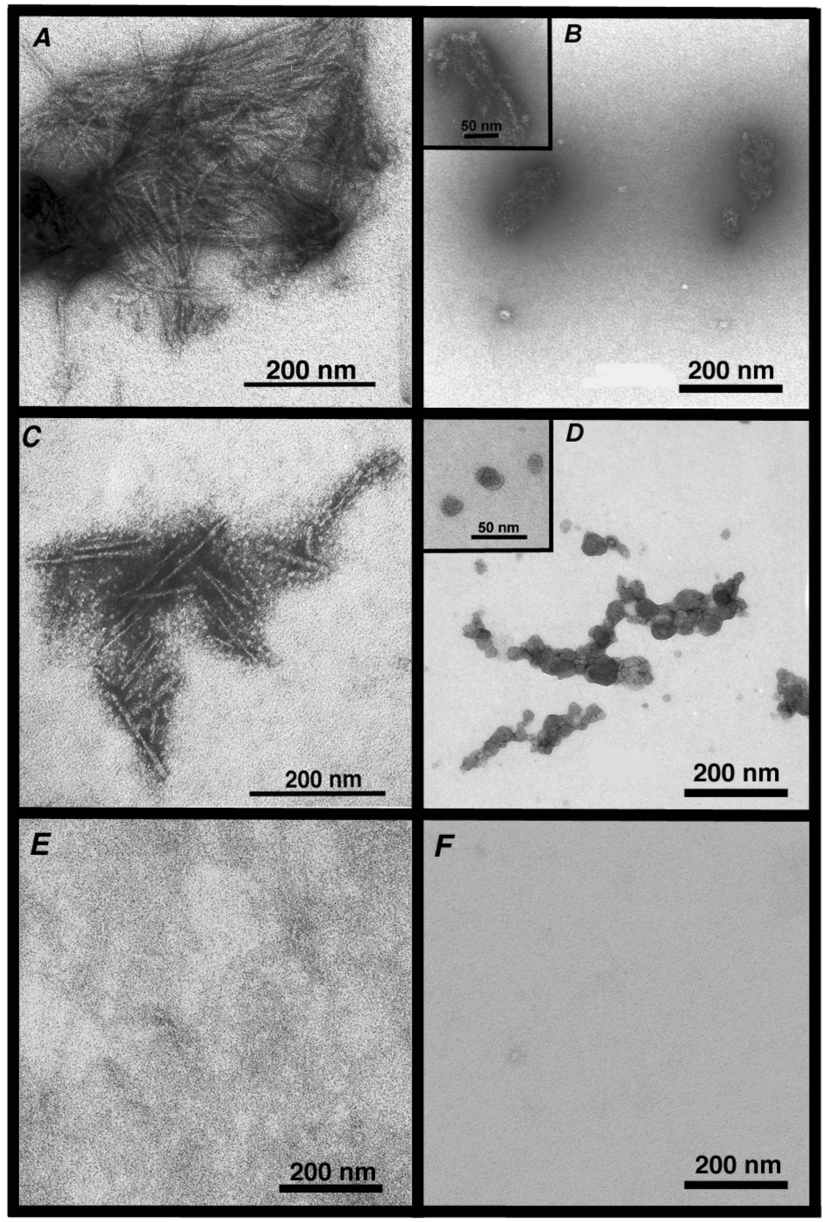

FIGURE 5: Transmission electron microscopy images of LC aggregates observed at pH 7.4. (A) κ-MJM (1 mg/mL) after 160 h of stirring at 37 °C with 4-HNE (100 μM). (B) κ-MJM (1 mg/mL) after 160 h of stirring at 37 °C with ALD (100 μM). (C) λ-L155 (1 mg/mL) after 160 h of stirring at 37 °C with 4-HNE (100 μM). (D) λ-L155 (1 mg/mL) after 160 h of stirring at 37 °C with ALD (100 μM). (E) κ-MJM (1 mg/mL) after 160 h of stirring at 37 °C with VEH. (F) λ-L155 (1 mg/mL) after 160 h of stirring at 37 °C with VEH.

and PUFA peroxidation, causes protein dysfunction via glycation of Lys, Arg, and Cys side chains. The reactivity of such aldehydes, when generated *in vivo*, is so high that it has been suggested that such lipidic aldehydes should not be seen as end products of lipid peroxidation processes but rather as "second toxic messengers" for the primary free radicals that spawn them (*49*).

The specific LCs used in this study were selected because they are members of the two main subclasses of antibody LCs, κ or λ, and are not linked to any incidence of LCDD. As described *vide infra*, there is as yet no clear way, based upon amino acid sequence, that allows one to predict whether an LC will form fibrils. Our hypothesis challenges that any LC, regardless of primary structure, if expressed in sufficiently high concentrations and when juxtaposed with inflammatory aldehydes of the appropriate structure and concentration will aggregate. Therefore, there was no specific need to utilize a known amyloidogenic or aggregation-prone LC for this study; rather we simply sought to investigate if a random LC could be induced to aggregate under the influence of inflammatory aldehydes. However, there was a pragmatic aspect to the selection of the light chain. To perform these experiments, we needed multimilligram amounts of essentially homogeneous protein, and for that we studied a κ light chain from an essentially monoclonal IgM from a lymphoma patient (from which we routinely isolated and purified hundreds of milligrams of LC) and a cloned human λ light chain in a cultured plasmacytoma cell line (which could be induced to generate tens of milligrams of light chain) (*24, 25*).

As is known for protein aggregation in general (*50*) and LCs specifically (*15, 51*), the rate of aggregation/fibrillization is highly sensitive to extrinsic physical factors, such as pH, agitation, temperature, and pressure. Some authors will, for

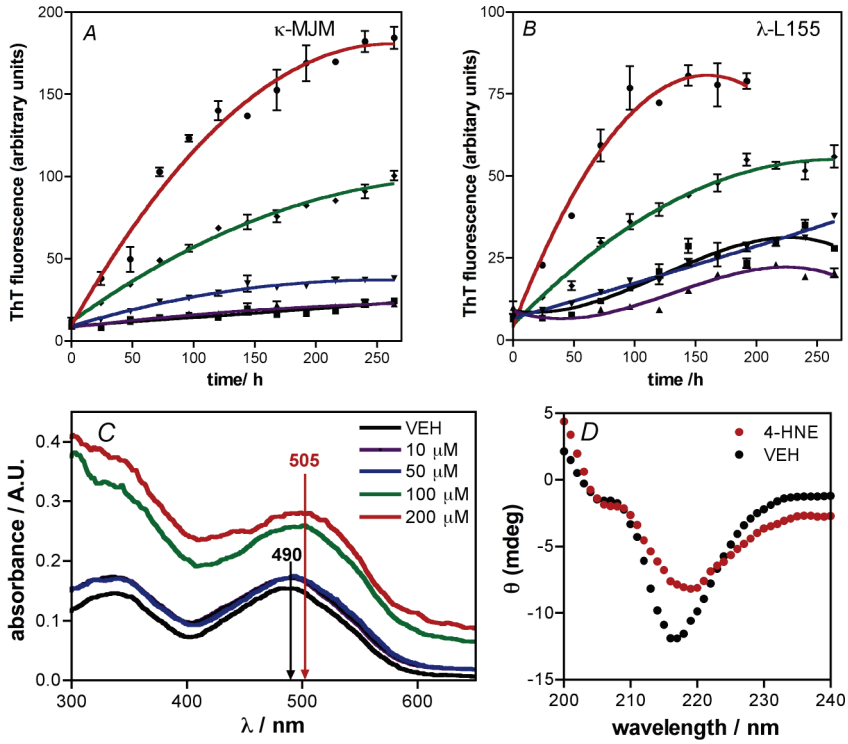

FIGURE 6: Effect of 4-HNE on aggregation of human AL. (A) ThT fluorescence of solutions of κ-MJM (1 mg/mL) at pH 7.4 during stirring at 37 °C with 4-HNE (10 μM, ▲; 50 μM, ▼; 100 μM, ◆; 200 μM, ●) or VEH (PBS, 0.1% IPA, ■). (B) ThT fluorescence of solutions of λ-L155 (1 mg/mL) at pH 7.4 during stirring at 37 °C with 4-HNE (10 μM, ▲; 50 μM, ▼; 100 μM, ◆; 200 μM, ●) or VEH (PBS, 0.1% IPA, ■). At times during the incubation, aliquots were removed, ThT was added (40 μM in water), the solution was incubated for 20 min, and then fluorescence readings were taken (excitation, 440 nm; emission, 485 nm). Each data point is reported as the mean ± SEM of duplicate measurements. (C) Spectral characteristics of Congo Red bound to κ-MJM (1 mg/mL) at pH 7.4 during stirring at 37 °C for 160 h after incubation with 4-HNE (10 μM, purple line; 50 μM, blue line; 100 μM, green line; 200 μM, red line) or VEH (PBS, 0.1% IPA, black line). Absorbance spectra (300−625 nm) of solutions of CR (81 μM) and κ-MJM (0.09 mg/mL) are uncorrected. (D) Far-UV circular dichroism spectra for κ-MJM (1 mg/mL) after incubation with either 4-HNE (100 μM, red circles) or VEH (PBS, 0.1% IPA, black circles) at 37 °C for 100 h.

example, use LC's that did not form amyloid depositions in myeloma patients to specific denaturing conditions to generate fibrils *in vitro* in order to learn more about early events in aggregation (*52*). In order to maximize the relevance of the observation in these experiments, the physical conditions exploited throughout this study were designed to mimic as closely as possible a physiological environment. Thus, aggregation assays were performed in phosphate-buffered saline, pH 7.4 and 37 °C, with mild agitation. The only nonphysiologic condition was the inclusion of IPA (0.1% v/v) to increase the aqueous solubility of some of the aldehydes being studied. Control aggregation assays with the two light chains κ-MJM and λ-L155 at 43 μM in VEH (PBS, pH 7.4, 0.1% IPA) revealed that these two LCs are very stable, with no aggregation being detected at up to 350 h under these conditions (Figures 2F and 4). For comparison, Fink and co-workers have shown that the amyloidogenic V_L SMA under similar aggregation conditions (40 μM, pH 7.0, 37 °C with stirring) aggregates with a lag phase (measured by extrapolation of the logarithmic growth phase to zero) of ~250 h. Interestingly, when the λ-L155 concentration was increased to 2 mg/mL and the aggregation studied with VEH under otherwise identical conditions, evidence of a nucleated-type amyloidogenesis was obtained by ThT fluorescence (Figure 6B), a lag phase of ~100 h being observed.

In this study we reproducibly observe that a panel of aldehydes that trace their *in vivo* origins to oxidation of PUFAs (4-HNE, MDA, and GLY) and cholesterol (KA and ALD) can, upon complexation with human antibody light chains (either κ- or λ-isotypes) *in vitro*, accelerate the misfolding and aggregation of these antibody LCs. ThT, CR binding, and turbidity analyses reveal that 4-HNE, MDA, and GLY induce aggregates with increased β-sheet conformation in both the κ-MJM and λ-L155 proteins, whereas KA and ALD accelerate the formation of amorphous aggregates in the κ-MJM light chain.

There is an increasing body of evidence to suggest that protein aggregation, which includes amyloid and non-amyloid processes, arises from kinetically accessible partially folded conformers (*53, 54*). Fink and co-workers (*55*) have recently applied this hypothesis to explain the aggregation of the AL-protein, SMA, which can form both amorphous and fibrillar aggregates. Our *in vitro* aggregation data and TEM morphological analyses with the κ-MJM and λ-L155 light chains add further support for this hypothesis, as both light chains are able to form different structural aggregates, either fibrillar or amorphous, dependent upon the aldehyde to which they are exposed (Figure 5). Such a working hypothesis also offers a hint as to how different inflammatory aldehydes may trigger the formation of different aggregates from the same globular protein (Figure 8). The primary assumption is that there are two accessible intermediate protein conformations, I_A and I_B, available from the native structure N and that non-amyloid aggregates are accessible from I_A and amyloid aggregates are accessible from I_B. The role then for the specific aldehyde would be to adduct to the lysine side chains and bind to

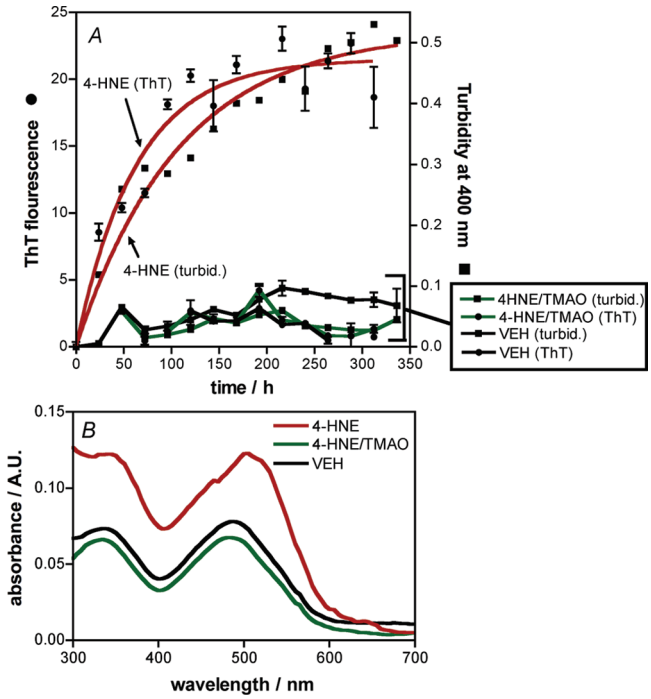

FIGURE 7: Trimethylamine *N*-oxide prevents 4-HNE-induced aggregation of κ-MJM. (A) Aggregation of human LC κ-MJM as measured by ThT fluorescence (left *Y*-axis) and turbidity (right *Y*-axis). The human AL-κ-MJM (1 mg/mL, 42 μM) in PBS (pH 7.4) was incubated at 37 °C with either 4-HNE at 100 μM (red line), 4-HNE at 100 μM with TMAO at 500 μM (green line), or VEH (black line). At times throughout the assay, aliquots were removed, and either the aliquots were added to a ThT solution (20 μM) in water and the fluorescence was measured (excitation, 440 nm; emission, 485 nm) or the turbidity of the solution was measured (400 nm). Data are reported as the mean ± SEM for at least duplicate measurements. (B) Spectral characteristics of Congo Red bound to κ-MJM (1 mg/mL) at pH 7.4 during stirring at 37 °C for 100 h after incubation with 4-HNE at 100 μM (red line), 4-HNE with TMAO at 500 μM (green line), or VEH (black line). Absorbance spectra (300−700 nm) of final solutions of CR (81 μM) and κ-MJM (0.09 mg/mL) were uncorrected.

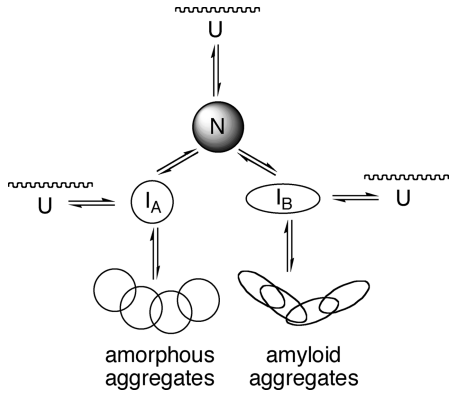

FIGURE 8: Hypothetical relationship between the native folded state of an antibody light chain N and different partially folded secondary structural intermediates I_A and I_B on a pathway to either amorphous or amyloid aggregates, respectively. The completely unfolded state U is shown as being accessible from N, I_A, and I_B.

complementary sites, presumably hydrophobic domains due to the hydrophobic nature of the aldehydes, on the protein that facilitate either formation of intermediates I_A or I_B or conversion of these intermediates into their corresponding aggregates. The *in vitro* aggregation assays in these studies were designed to ensure that at the start of the experiments the light chains were in their native globular form N; for this reason, the experiments were performed under physiological conditions, PBS at pH 7.4, and not under artificial conditions that would intrinsically destabilize N, such as low pH.

The mole equivalents of aldehyde to protein that are sufficient to accelerate the aggregation of the LC is very low. All the screening aggregation assays with the aldehydes employed an equilibrium molar ratio of 2.2 aldehyde to 1 protein, and in all cases this ratio was sufficient to significantly accelerate LC protein aggregation (Figure 2). The concentration dependence of 4-HNE in the aggregation of κ-MJM (80 μM) revealed a clear acceleration in the protein aggregation rate at 0.625 mol equiv of 4-HNE to κ-MJM (Figure 6A). As the mole equivalents of aldehyde to κ-MJM increased, so did the aggregation rate and so did the amount of β-sheet-containing aggregate, as determined by the absolute ThT fluorescence. The concentration dependence of 4-HNE in the aggregation of λ-L155 (80 μM) showed only a clear acceleration in the protein aggregation rate at 1.25 mol equiv of 4-HNE to λ-L155 (Figure 6B). But, as shown for κ-MJM, as the mole equivalents of aldehyde to λ-L155 increased, so did the aggregation rate and so did the amount of β-sheet-containing aggregate. What these data suggest is that a protein−aldehyde complex of only 1:1 could be sufficient to give rise to a productive proaggregation conformation. This is a truly remarkable finding given that the molecular weight of both the human ALs, κ-MJM and λ-L155, is ~ 25000 and 4-HNE is only 156. At the molecular level, there will be a change in the net surface charge of the protein of −1 and a structural modification of one Lys side chain into a lipid side chain.

The fact that TMAO (500 μM) protects the antibody light chain from the effect of the 4-HNE adduction is informative for a number of reasons. First, it is supportive of the working hypothesis proposed in Figure 8, because in line with what is the accepted role of such chemical chaperones, TMAO should preferentially stabilize the light chains in their native conformation N, thus minimizing the equilibrium concentration of the intermediates, I_A and I_B, and hence aldehyde-induced access to the misfolded aggregates. Also, it is also suggestive that TMAO and other chemical chaperones may well have application as therapeutic approaches to LC amyloidosis and LCDD, a fact that has, to our knowledge, never before been reported.

Based on the results reported here, it is now important to assess whether inflammatory aldehydes are contributing to LC deposition diseases *in vivo*. One can imagine hypothetically how this inflammatory aldehyde triggered aggregation phenomenon may contribute to LC disease *in vivo*. For example, in cases where one has elevated circulating levels of a light chain in multiple myeloma, then in the case of an acute inflammation, there would be elevated levels of aldehydes, either systemic or localized, and this increase could trigger the aggregation and deposition of the circulating light chain. It should also be noted that, in contrast to what has been observed with the localization of the GAGs within LC amyloid deposits (*19, 56*), there would be no expectation that the aldehydes having seeded the LC deposition would necessarily be detectable within the deposit. The nature of the chemical interaction between the aldehyde and the lysine side chains

is covalent but reversible, and thus the process could essentially be traceless. However, if the aldehyde-induced aggregation were occurring *in vivo*, then a therapeutic approach based upon chemical chaperones, as we have shown to be effective *in vitro* with TMAO, would be an important starting point for investigation.

In conclusion, we have shown that a panel of lipid aldehydes can accelerate antibody light chain aggregation *in vitro*. We have shown that specific aldehydes can trigger misfolding that is characterized by increased β-sheet secondary protein structure and that the effects of aldehydes on structure are independent of antibody isotype. We have also shown that this phenomenon of aldehyde-accelerated light chain aggregation can be blocked by the presence of a chemical chaperone, TMAO. Translation of these *in vitro* results into the possible *in vivo* relevance of inflammatory aldehyde induced LCDD or AL-amyloidosis is something we are studying intensively and will be reported in due course.

ACKNOWLEDGMENT

The authors thank all members of the Wentworth laboratory (TSRI) for assistance and suggestions during this work, Dr. Andrew King (Scripps Clinic) for providing the MM patient plasma, Mr. David Kujawa (TSRI) for assistance in light chain purification, Prof. Reza Gadhiri for access to his CD machine, and Mr. Malcolm Wood for EM images.

REFERENCES

1. Buxbaum, J. (1992) Mechanisms of disease: monoclonal immunoglobulin deposition. Amyloidosis, light chain deposition disease, and light and heavy chain deposition disease. *Hematol. Oncol. Clin. North Am. 6*, 323–346.
2. Buxbaum, J. N., Chuba, J. V., Hellman, G. C., Solomon, A., and Gallo, G. R. (1990) Monoclonal immunoglobulin deposition disease: light chain and light and heavy chain deposition diseases and their relation to light chain amyloidosis. Clinical features, immunopathology, and molecular analysis. *Ann. Intern. Med. 112*, 455–464.
3. Pelegri, A., Campo, E., Romero, R., Reguant, M., and Aisa, L. (1986) AL-type amyloidosis and light chain deposition disease. *Clin. Nephrol. 25*, 220.
4. Gertz, M. A., Lacy, M. Q., and Dispenzieri, A. (1999) Amyloidosis. *Hematol. Oncol. Clin. North Am. 6*, 1211–1233.
5. Glenner, G. G., Harbaugh, J., Ohms, J. I., Harada, M., and Cuatrecasas, P. (1970) An amyloid protein: the amino-terminal variable fragment of an immunoglobulin light chain. *Biochem. Biophys. Res. Commun. 41*, 1287–1289.
6. Glenner, G. G. (1980) Amyloid deposits and amyloidosis. The beta-fibrilloses (first of two parts). *N. Engl. J. Med. 302*, 1283–1292.
7. Bellotti, V., Mangione, P., and Merlini, G. (2000) Review: immunoglobulin light chain amyloidosis-the archetype of structural and pathogenic variability. *J. Struct. Biol. 130*, 280–289.
8. Hsu, J. Y., Shu, K. H., Chan, L. P., Lu, Y. S., Cheng, C. H., Sheu, S. S., and Lian, J. D. (1994) The clinicopathological spectrum of renal amyloidosis. *Zhonghua Yixue Zazhi (Taipei, Taiwan) 54*, 230–239.
9. Preud'homme, J. L., Aucouturier, P., Touchard, G., Khamlichi, A. A., Rocca, A., Denoroy, L., and Cogne, M. (1994) Monoclonal immunoglobulin deposition disease: a review of immunoglobulin chain alterations. *Int. J. Immunopharmacol. 16*, 425–431.
10. Kyle, R. A. (1989) Monoclonal gammopathies and the kidney. *Annu. Rev. Med. 40*, 53–60.
11. Solomon, A., Weiss, D. T., and Wall, J. S. (2003) Immunotherapy in systemic primary (AL) amyloidosis using amyloid-reactive monoclonal antibodies. *Cancer Biother. Radiopharm. 18*, 853–860.
12. Gallo, G., Picken, M., Buxbaum, J., and Frangione, B. (1989) unknown. *Semin. Hematol. 26*, 234–245.
13. Ganeval, D., Nöel, L.-H., Preud'homme, J. L., Droz, D., and Grünfeld, J.-P. (1984) unknown. *Kidney Int. 26*, 1–9.
14. Kaplan, B., Vidal, R., Kumar, A., Ghiso, J., Frangione, B., and Gallo, G. (1997) Amino-terminal identity of co-existent amyloid and non-amyloid immunoglobulin kappa light chain deposits. A human disease to study alterations of protein conformation. *Clin. Exp. Immunol. 110*, 472–478.
15. Wall, J., Schell, M., Murphy, C., Hrncic, R., Stevens, F. J., and Solomon, A. (1999) Thermodynamic instability of human lambda 6 light chains: correlation with fibrillogenicity. *Biochemistry 38*, 14101–14108.
16. Ozaki, S., Abe, M., Wolfenbarger, D., Weiss, D. T., and Solomon, A. (1994) Preferential expression of human lambda-light-chain variable-region subgroups in multiple myeloma, AL amyloidosis, and Waldenstrom's macroglobulinemia. *Clin. Immunol. Immunopathol. 71*, 183–189.
17. Solomon, A., and Weiss, D. T. (1987) Serologically defined V region subgroups of human lambda light chains. *J. Immunol. 139*, 824–830.
18. Hurle, M. R., Helms, L. R., Li, L., Chan, W., and Wetzel, R. (1994) A role for destabilizing amino acid replacements in light-chain amyloidosis. *Proc. Natl. Acad. Sci. U.S.A. 91*, 5446–5450.
19. Stevens, F. J., and Kisilevsky, R. (2000) Immunoglobulin light chains, glycosaminoglycans, and amyloid. *Cell. Mol. Life Sci. 57*, 441–449.
20. Wentworth, P., Jr., Nieva, J., Takeuchi, C., Galve, R., Wentworth, A. D., Dilley, R. B., DeLaria, G. A., Saven, A., Babior, B. M., Janda, K. D., Eschenmoser, A., and Lerner, R. A. (2003) Evidence for ozone formation in human atherosclerotic arteries. *Science 302*, 1053–1056.
21. Zhang, Q., Powers, E. T., Nieva, J., Huff, M. E., Dendle, M. A., Bieschke, J., Glabe, C. G., Eschenmoser, A., Wentworth, P., Jr., Lerner, R. A., and Kelly, J. W. (2004) Metabolite-initiated protein misfolding may trigger Alzheimer's disease. *Proc. Natl. Acad. Sci. U.S.A. 101*, 4752–4757.
22. Scheinost, J. C., Wang, H., Boldt, G. E., Offer, J., and Wentworth, P. J. (2008) Cholesterol seco-sterol-induced aggregation of methylated amyloid-102 peptides—Insights into aldehyde-initiated fibrillization of amyloid-β, Angew. Chem., Int. Ed. (in press).
23. Bosco, D. A., Fowler, D., Zhang, Q., Nieva, J., Powers, E. T., Wentworth, J., P., Lerner, R. A., and Kelly, J. W. (2006) Toxic cholesterol metabolites that are elevated in Lewy body disease brains accelerate alpha-synuclein fibrillization in vitro. *Nat. Chem. Biol. 2*, 249–253.
24. Matsuoka, Y., Yagi, Y., Moore, G. E., and Pressman, D. (1969) Isolation and characterization of free lambda-chain of immunoglobulin produced by an established cell line of human myeloma cell origin. II. Identity of lambda-chains in cells and in medium. *J. Immunol. 103*, 962–969.
25. Moore, G. E., and Kitamura, H. (1968) Cell line derived from patient with myeloma. *N.Y. State J. Med. 68*, 2054–2060.
26. Klunk, W. E., Jacob, R. F., and Mason, R. P. (1999) Quantifying amyloid β-peptide (aβ) aggregation using the Congo Red-Aβ (CR-Aβ) spectrophotometric assay. *Anal. Biochem. 266*, 66–76.
27. Lobley, A., and Wallace, B. A. (2001) DICHROWEB: a website for the analysis if protein secondary structure from circular dichroism spectra. *Biophys. J. 80*, 373a.
28. Lobley, A., Whitmore, L., and Wallace, B. A. (2002) DICHROWEB: an interactive website for the analysis of protein secondary structure from circular dichroism spectra. *Bioinformatics 18*, 211–212.
29. Manavalan, P., and Johnson, W. C. J. (1986) Variable selection method improves the prediction of protein secondary structure from circular dichroism spectra. *Anal. Biochem. 167*, 76–85.
30. Sreerema, N., and Woody, R. W. (1993) A self-consistent method for the analysis of protein secondary structure from circular dichroism. *Anal. Biochem. 209*, 32–44.
31. LeVine, I. I. I. H., and Ronald, W. (1999) Quantification of β-sheet amyloid fibril structures with thioflavin T, in *Methods in Enzymology*, pp 274−284, Academic Press, New York.
32. Hurshman, A. R., White, J. T., Powers, E. T., and Kelly, J. W. (2004) Transthyretin aggregation under partially denaturing conditions is a downhill polymerization. *Biochemistry 43*, 7365–7381.
33. Ferrone, F. (1999) Analysis of protein aggregation kinetics. *Methods Enzymol. 309*, 256–274.

34. Oosawa, F., and Asakura, S. (1975) *Thermodynamics of the Polymerization of Protein*, Academic Press, London.
35. Kihara, M., Chatani, E., Sakai, M., Hasegawa, K., Naiki, H., and Goto, Y. (2005) Seeding-dependent maturation of beta2-microglobulin amyloid fibrils at neutral pH. *J. Biol. Chem. 280*, 12012–12018.
36. Perlmutter, D. H. (2002) Chemical chaperones: A pharmacological strategy for disorders of protein folding and trafficking. *Pediatr. Res. 52*, 832–836.
37. Tazelt, J., Prusiner, S. B., and Welch, W. J. (1996) Chemical chaperones interfere with the formation of scrapie prion protein. *EMBO J. 15*, 6363–6373.
38. Bennion, B. J., DeMarco, M. L., and Daggert, V. (2004) Preventing misfolding of the prion protein by trimethylamine N-oxide. *Biochemistry 43*, 12595–12963.
39. Esterbauer, H. (1982) Lipid peroxidation products: formation, chemical properties and biological activities, in *Free Radical in Liver Injury* (Poli, G., Cheeseman, K. H., Dianzani, M. U., and Slater, T. F., Eds.) pp29−47, IRL Press, Oxford.
40. Benedetti, A., Comporti, M., and Esterbauer, H. (1980) Identification of 4-hydroxynonenal as a cytotoxic product originating from the peroxidation of liver microsomal lipids. *Biochim. Biophys. Acta 620*, 281–296.
41. Zarkovic, K. (2003) 4-Hydroxynonenal and neurodegenerative diseases. *Mol. Aspects Med. 24*, 293–303.
42. Tamagno, E., Parola, M., Bardini, P., Piccini, A., Borghi, R., Guglielmotto, M., Santoro, G., Davit, A., Danni, O., Smith, M. A., Perry, G., and Tabaton, M. (2005) Beta-site APP cleaving enzyme up-regulation induced by 4-hydroxynonenal is mediated by stress-activated protein kinases pathways. *J. Neurochem. 92*, 628–636.
43. Tamagno, E., Robino, G., Obbili, A., Bardini, P., Aragno, M., Parola, M., and Danni, O. (2003) H_2O_2 and 4-hydroxynonenal mediate amyloid beta-induced neuronal apoptosis by activating JNKs and p38MAPK. *Exp. Neurol. 180*, 144–155.
44. Leonarduzzi, G., Robbesyn, F., and Poli, G. (2004) Signaling kinases modulated by 4-hydroxynonenal. *Free Radical Biol. Med. 37*, 1694–1702.
45. Escargueil-Blanc, I., Salvayre, R., Vacaresse, N., Jurgens, G., Darblade, B., Arnal, J.-F., Parthasarathy, S., and Negre-Salvayre, A. (2001) Mildly oxidized LDL induces activation of platelet-derived growth factor β-receptor pathway. *Circulation 104*, 1814–1821.
46. McGrath, L. T., McGleenon, B. M., Brennan, S., McColl, D., McIlroy, S., and Passmore, A. P. (2001) Increased oxidative stress in Alzheimer's disease as assessed with 4-hydroxynonenal but not malondialdehyde. *QJM: Mon. J. Assoc. Physicians 94*, 485–490.
47. Grune, T., Michel, P., Sitte, N., Eggert, W., Albrecht-Nebe, H., Esterbauer, H., and Siems, W. (1997) Increased levels of 4-hydroxynonenal modified proteins in plasma of children with autoimmune diseases. *Free Radical Biol. Med. 23*, 357–360.
48. Przekwas, M., Malgorzewicz, S., Zdrojewski, Z., Debska-Slizien, A., Lysiak-Szydlowska, W., and Rutkowski, B. (2003) Influence of predialysis oxidative stress on peroxidation processes after renal transplantation. *Transplant Proc. 35*, 2170–2173.
49. Esterbauer, H., Zollner, H., and Schaur, R. J. (1990) Aldehydes formed by lipid peroxidation: mechanisms of formation, occurrence, and determination, in *Membrane Lipid Oxidation* (Vigo-Pelfrey, C., Ed.) pp239−268, CRC Press, Boston, MA.
50. Buxbaum, J. N. (2003) Diseases of protein conformation: what do in vitro experiments tell us about in vivo diseases? *Trends Biochem. Sci. 28*, 585–592.
51. Khurana, R., and Fink, A. L. (2000) Do parallel beta-helix proteins have a unique Fourier transform infrared spectrum? *Biophys. J. 78*, 994–1000.
52. Souillac, P. O., Uversky, V. N., Millett, I. S., Khurana, R., Doniach, S., and Fink, A. L. (2002) Elucidation of the molecular mechanism during the early events in immunoglobulin light chain amyloid fibrillation. Evidence for an off-pathway oligomer at acidic pH. *J. Biol. Chem. 277*, 12666–12679.
53. Booth, D. R., Sunde, M., Belloti, V., Robinson, C. V., Hutchinson, W. L., Fraser, P. E., Hawkins, P. N., Dobson, C. M., Radford, S. E., Blake, C. C. F., and Pepys, M. B. (1997) Instability, unfolding and aggregation of human lysozyme variants underlying amyloid fibrillogenesis. *Nature 385*, 787–793.
54. Wetzel, R. (1996) For protein misassembly, it's the I decade. *Cell 86*, 699–702.
55. Khurana, R., Gillespie, J. R., Talapatra, A., Minert, L. J., Ionescu-Zaneti, C., Millett, I., and Fink, A. L. (2001) Partially folded intermediates as critical precursors of light chain amyloid fibrils and amorphous aggregates. *Biochemistry 40*, 3525–3535.
56. Jiang, X., Myatt, E., Lykos, P., and Stevens, F. J. (1997) Interaction between glycosaminoglycans and immunoglobulin light chains. *Biochemistry 36*, 13187–13194.

BI800333S